Supporting Information

HDAC1 overexpression reduces chemosensitivity by promoting cell survival and inhibiting apoptotic responses in Luminal A breast cancer cells

Yuqian Hu [1], Tingting Lyu [2, #], Xianyun Ji [3], Jing Gao [1], Zhaoyan Qiang [4, *] and Jianhong Zhang [1, *].

[1] Pharmacy Department, Tianjin Fourth Central Hospital, No. 3 Zhongshan Road, Hebei District, Tianjin 300143, China.

[2] Chinese Academy of Medical Sciences, Peking Union Medical College, No. 9 Dongdan Santiao, Dongcheng District, Beijing 100730, China.

[3] Department of Pediatrics, Shanxi Medical University, Yingze Campus, No. 56 Xinjian South Road, Yingze District, Taiyuan City, Shanxi Province, 030001, China.

[4] Department of Pharmacology, College of Basic Medical, Tianjin Medical University, No. 22 Qixiangtai Road, Heping District, Tianjin, 300070, China.

[#]Yuqian Hu and Tingting Lyu should be considered joint first author.

*Correspondence authors. Emails:

Professor Jianhong Zhang: Zhang_jianhong66@sina.com

Professor Zhaoyan Qiang: qzyss1@163.com

Contributing authors: huyuqian0622@126.com; lvtingting1224@163.com; jixianyun2022@163.com; 1030412407@qq.com

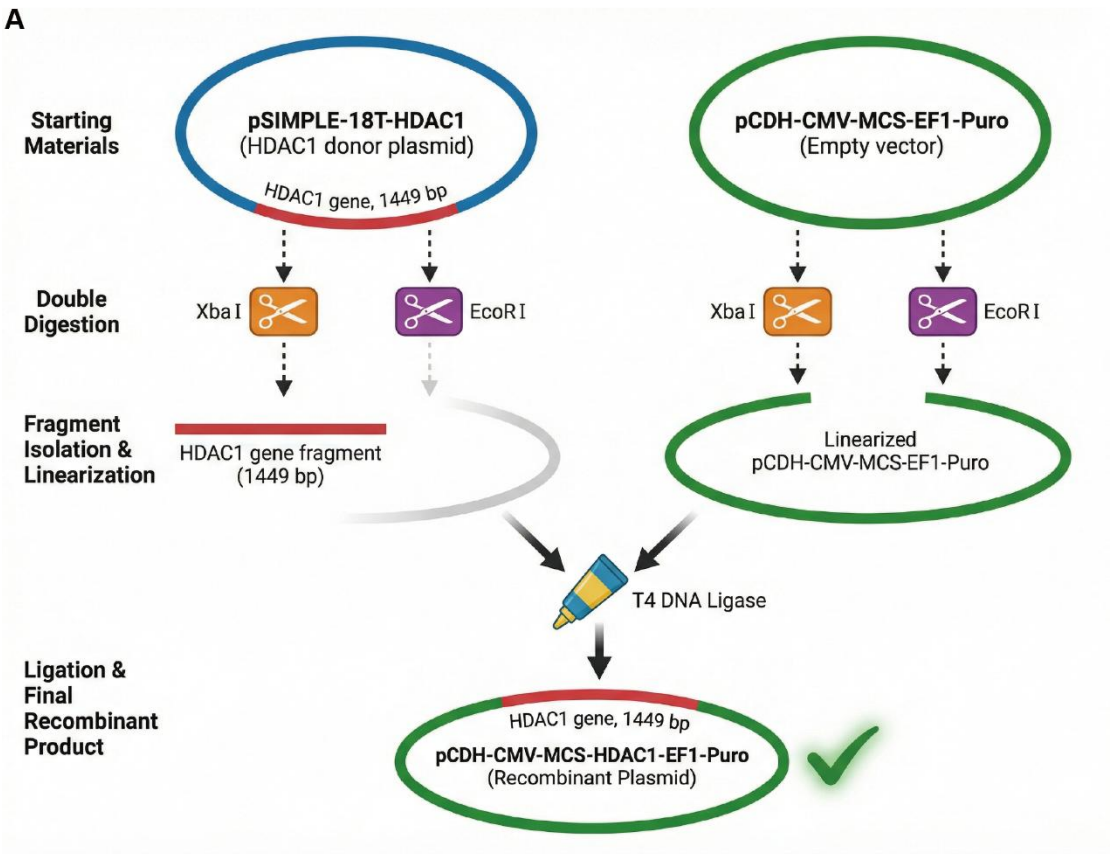
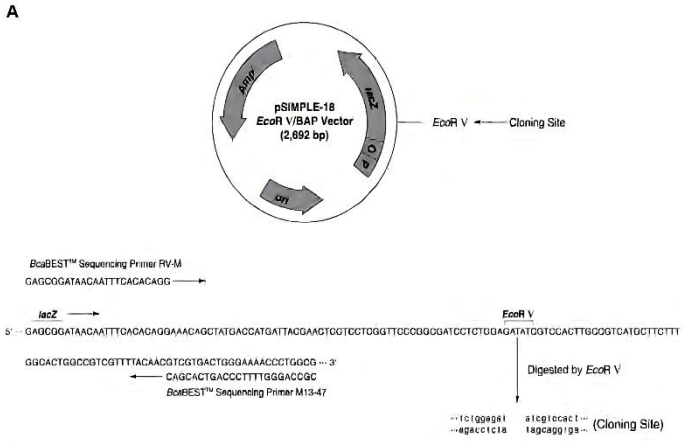


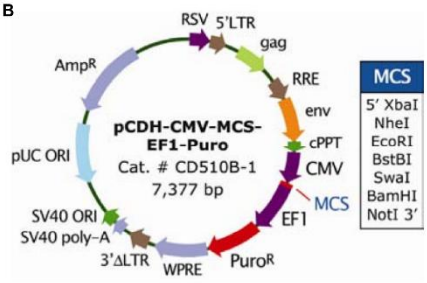
Figure S1. Map of the lentiviral packaging plasmids

(A) Schematic of pCDH-CMV-MCS-HDAC1-EF1-Puro construction by subcloning HDAC1 from pSIMPLE-18 into pCDH-CMV-MCS-EF1-Puro. **(B)** Representative sequencing chromatogram of the recombinant lentiviral vector pCDH-CMV-MCS-HDAC1-EF1-Puro confirming accurate insertion of the full-length HDAC1 coding sequence. Alignment of the HDAC1 sequencing results with the NCBI reference sequence demonstrating high sequence concordance and confirming the integrity of the cloned construct.

A

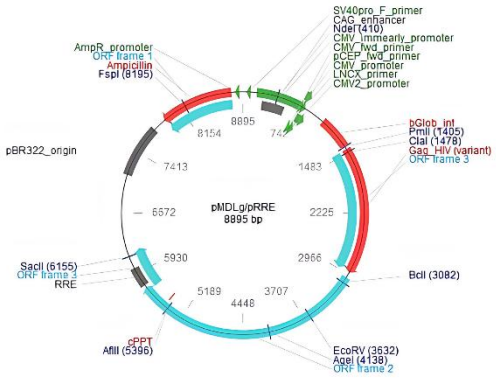


B

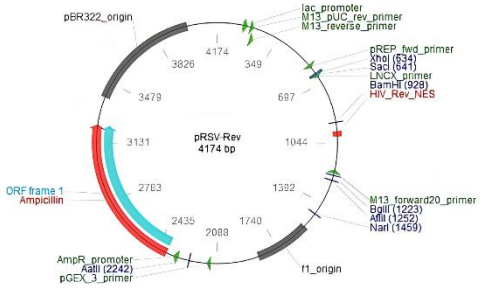


Features	
RSV:	7 - 234
5'LTR:	235 - 414
Gag:	567 - 919
RRE:	1076 - 1308
Env:	1309 - 1797
cPPT:	1798 - 1916
CMV:	1922 - 2271
EF1:	2315 - 2860
PuroR:	2866 - 3462
WPRE:	3472 - 4062
3ΔLTR:	4134 - 4367
SV40polyA:	4439 - 4570
SV40 ORI:	4579 - 4725
pUC ORI:	5095 - 5768(c)
AmpR:	5913 - 6773(c)
5'LTR-to-3'LTR:	4,132 bp

C



D



E

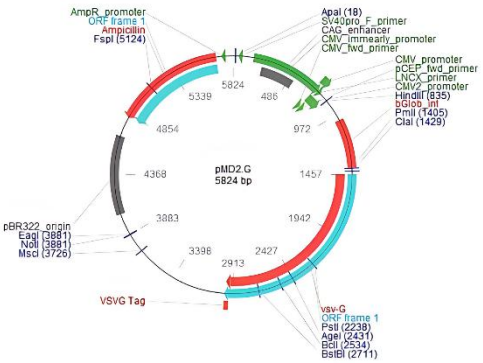


Figure S2. Construction of the HDAC1 lentiviral expression vector

(A) Map of the pSIMPLE-18 EcoR V/BAP vector used for cloning of the HDAC1 coding sequence. **(B)** Map of the pCDH-CMV-MCS-EF1-Puro lentiviral backbone. **(C)** Map of the lentiviral packaging plasmids pMDLg/pRRE. **(D)**Map of the lentiviral packaging plasmids pRSV-Rev. **(E)** Map of the lentiviral packaging plasmids pMD2.G.

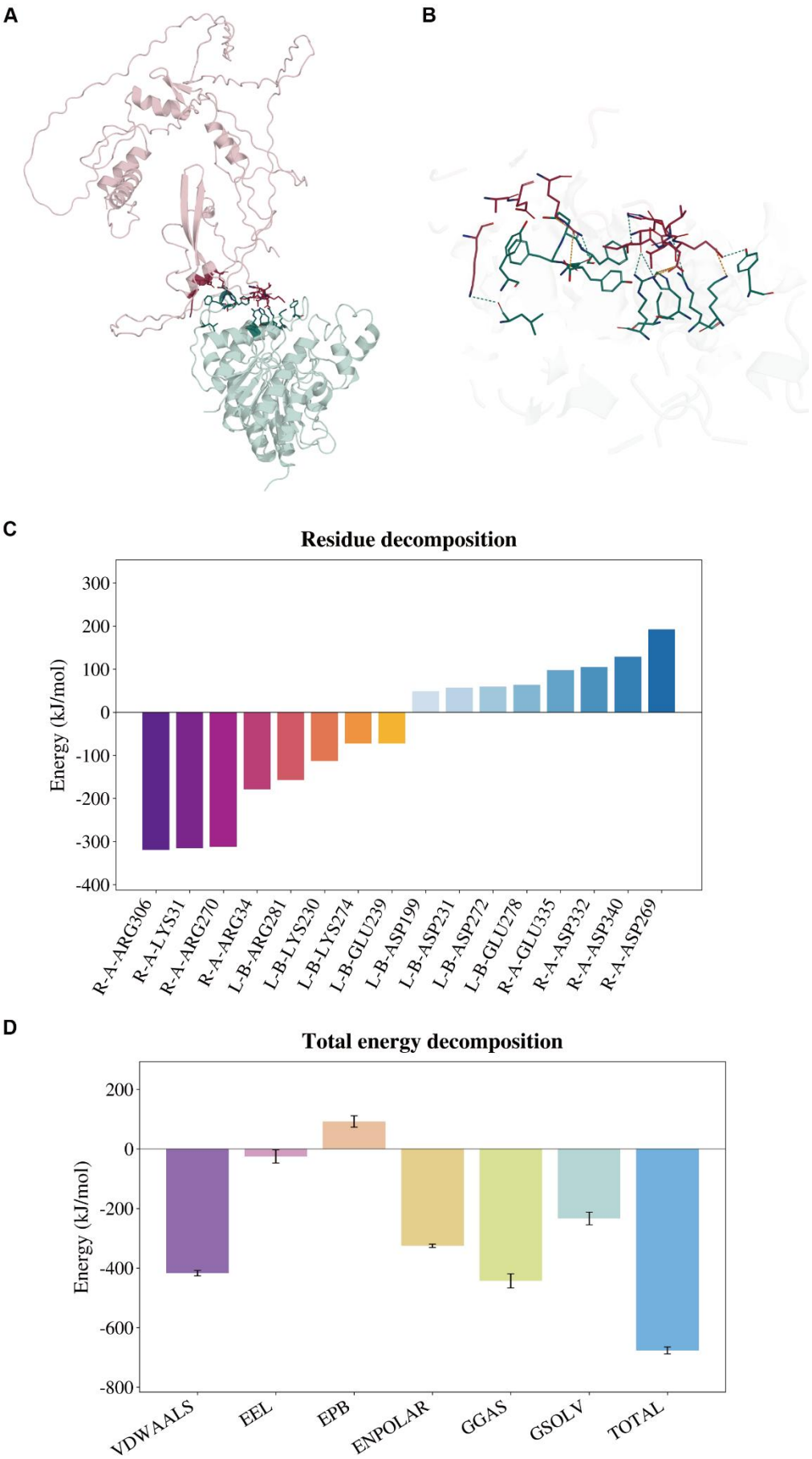

A
B
C
Residue decomposition
Energy (kJ/mol)
300
200
100
0
-100
-200
-300
-400
R-A-ARG306
R-A-LYS31
R-A-ARG270
R-A-ARG34
L-B-ARG281
L-B-LYS230
L-B-LYS274
L-B-GLU239
L-B-ASP199
L-B-ASP231
L-B-ASP272
L-B-GLU278
R-A-GLU335
R-A-ASP332
R-A-ASP340
R-A-ASP269
D
Total energy decomposition
Energy (kJ/mol)
200
0
-200
-400
-600
-800
VDWAALS
EEL
EPB
ENPOLAR
GGAS
GSOLV
TOTAL

Figure S3. Structural visualization and MM-PBSA energy decomposition of the HDAC1–YY1 complex.

(A) Overall three-dimensional structure of the predicted HDAC1–YY1 complex, showing the relative orientation of the two proteins at the binding interface. **(B)** Magnified view of the predicted interaction interface, highlighting the major intermolecular interactions between HDAC1 and YY1. **(C)** MM-PBSA energy decomposition of representative interface residues from Protein A (HDAC1) and Protein B (YY1), with negative values indicating favorable contributions to complex formation. **(D)** Decomposition of the total binding free energy into van der Waals (VDWAALS), electrostatic (EEL), polar solvation (EPB), non-polar solvation (ENPOLAR), molecular mechanics (GGAS), total solvation (GSOLV), and total binding free energy (TOTAL) components. Values are presented as mean ± SD.

Table S1. Summary of structural stability, residue-level energy contributions, and MM-PBSA binding energy of the HDAC1–YY1 complex.

Metric	Value
RMSD last 10% avg (nm)	1.458076
Rg last 10% avg (nm)	3.627594
SASA last 10% avg (nm^2)	403.179737
Hbond range (min-max)	4.0-21.0
RMSD mean (nm)	1.373861
Rg mean (nm)	3.832575
SASA mean (nm^2)	432.927396
RMSF high-fluctuation regions	Residues 432-446 (peak value: 1.525 nm)
Overall favorable residues (top 2, kJ/mol)	R-A-ARG306(-319.66 kJ/mol), R-A-LYS31(-315.30 kJ/mol)
Overall unfavorable residues (top 2, kJ/mol)	R-A-ASP269(192.51 kJ/mol), R-A-ASP340(128.78 kJ/mol)
Receptor favorable residues (top 2, kJ/mol)	R-A-ARG306(-319.66 kJ/mol), R-A-LYS31(-315.30 kJ/mol)
Receptor unfavorable residues	R-A-ASP269(192.51 kJ/mol),

(top 2, kJ/mol)	R-A-ASP340(128.78 kJ/mol)
Ligand favorable residues	L-B-ARG281(-157.17 kJ/mol),
(top 2, kJ/mol)	L-B-LYS230(-113.12 kJ/mol)
Ligand unfavorable residues	L-B-GLU278(63.68 kJ/mol),
(top 2, kJ/mol)	L-B-ASP272(59.57 kJ/mol)
VDWAALS (kJ/mol)	-417.61
EEL (kJ/mol)	-25.61
EPB (kJ/mol)	91.88
ENPOLAR (kJ/mol)	-325.52
GGAS (kJ/mol)	-443.21
GSOLV (kJ/mol)	-233.68
TOTAL (kJ/mol)	-676.89



Figure S4. Representative agarose gel electrophoresis of the PCR-amplified HDAC1 coding sequence, showing a single specific band at the expected size of 1449 bp.

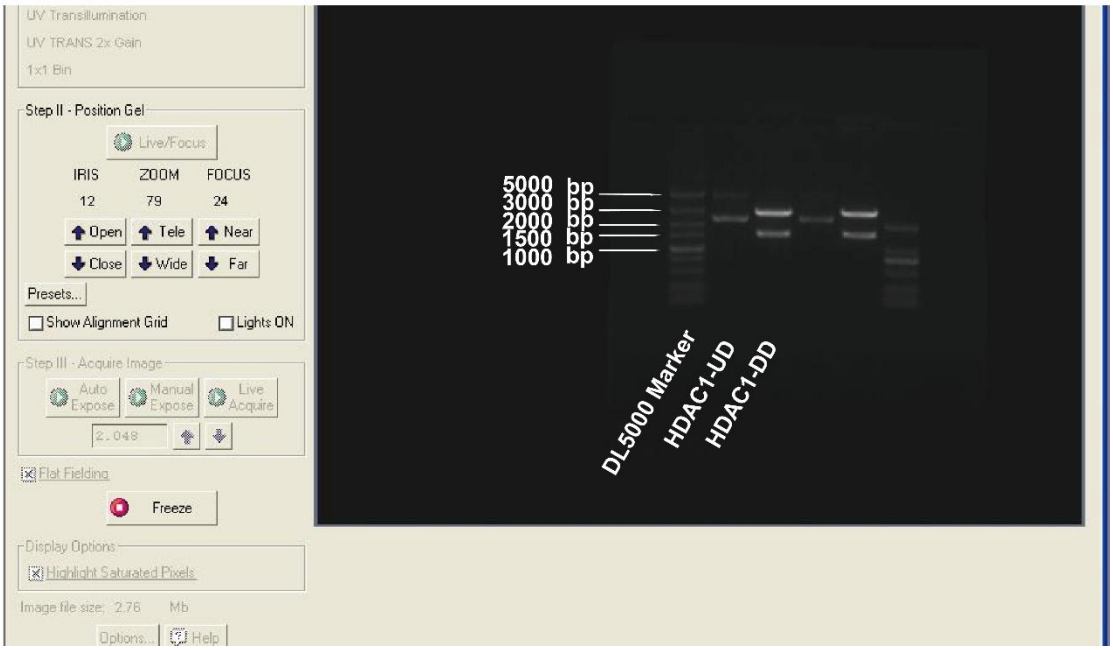


Figure S5. Agarose gel electrophoresis of the double-enzyme-digested recombinant pSIMPLE-18T–HDAC1 cloning vector, showing bands of approximately 2700 bp for the vector backbone and 1449 bp for the HDAC1 insert.

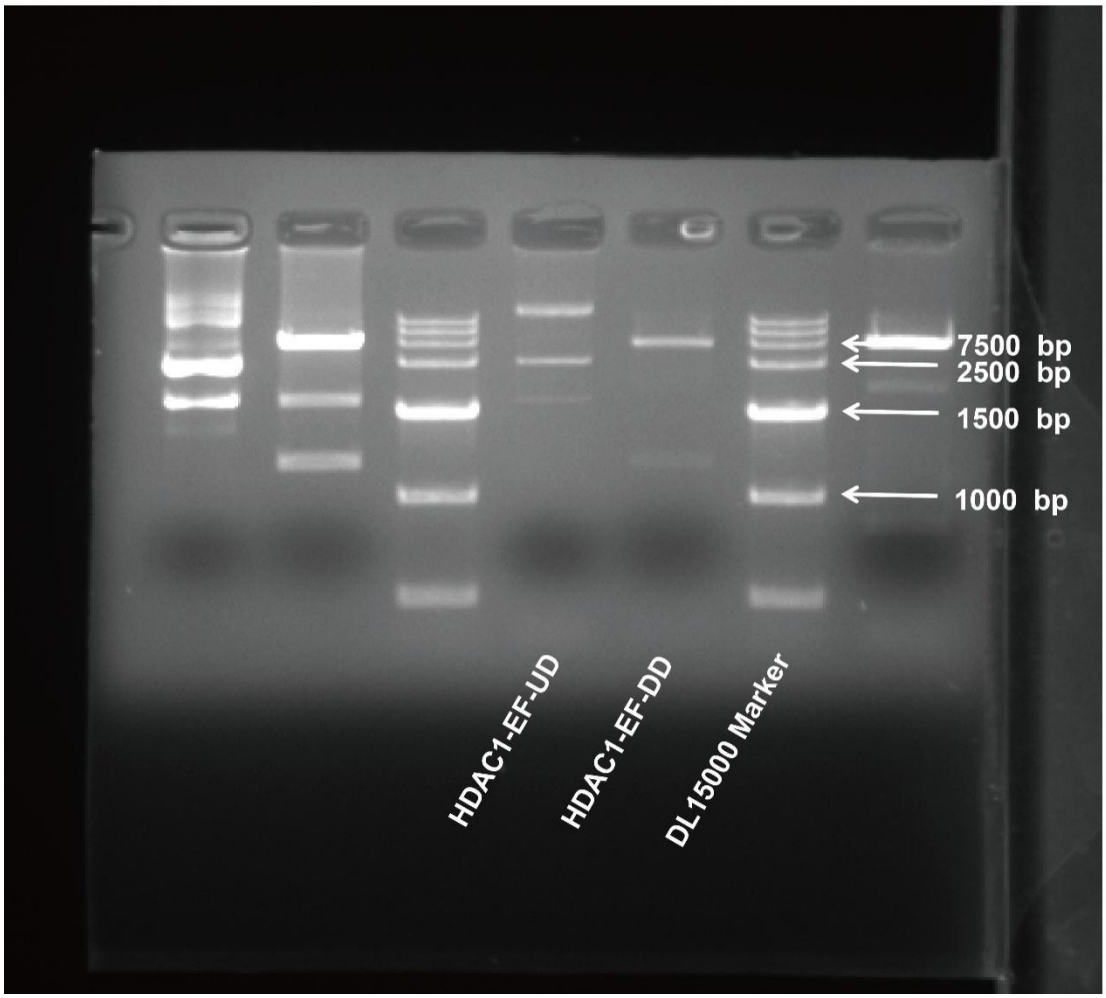


Figure S6. Agarose gel electrophoresis of the double-enzyme-digested recombinant pCDH-CMV-MCS-HDAC1-EF1-Puro lentiviral vector, showing bands of approximately 7400 bp corresponding to the vector backbone and 1449 bp corresponding to the HDAC1 insert.

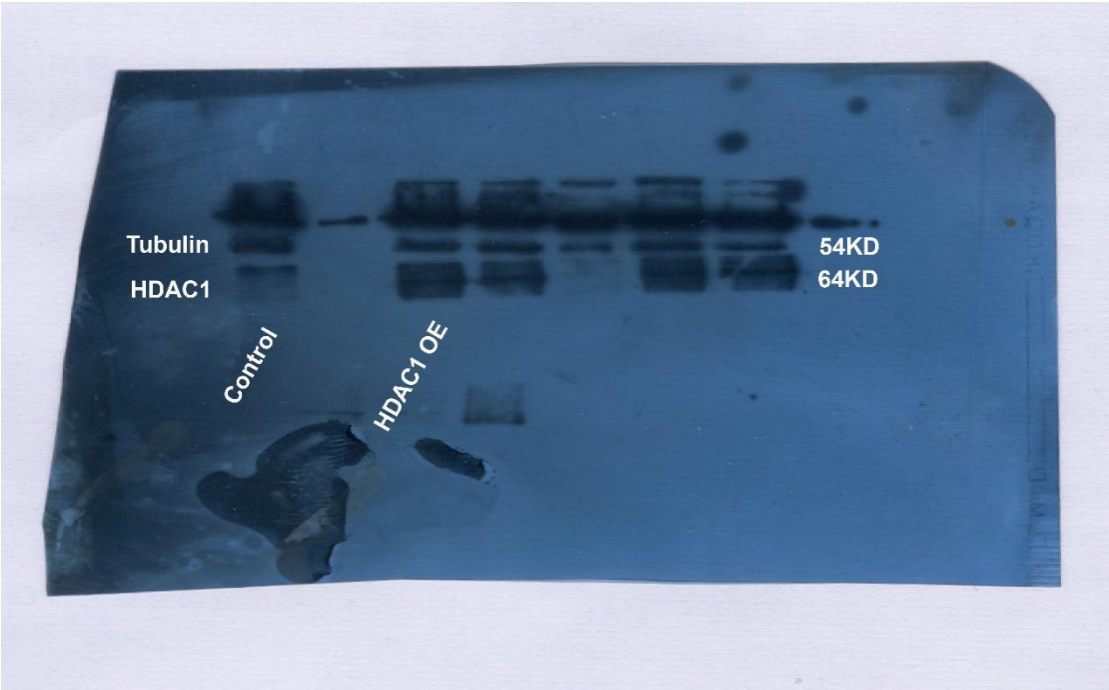


Figure S7. Western blot analysis of HDAC1 protein expression in MCF-7-Control and MCF-7-HDAC1 cells, with tubulin used as the loading control. HDAC1 expression was higher in MCF-7-HDAC1 cells than in MCF-7-Control cells.